



Decentralized robust tube-based model predictive control: application to a four-tank system

Control predictivo robusto descentralizado basado en tubos: aplicación a un sistema de cuatro tanques

F.D.J. Sorcia-Vázquez¹, C.D. Garcia-Beltran², G. Valencia-Palomo³, J.A. Brizuela-Mendoza¹,
J.Y. Rumbo-Morales^{1*}

¹Universidad de Guadalajara. Centro Universitario de los Valles. Carretera Guadalajara-Ameca Km.45.5 C.P. 46600, Ameca, Jalisco, México.

²Tecnológico Nacional de México, TecNM/CENIDET, Int. Internado Palmia S/N, Col. Palmira, Cuernavaca C.P. 62490, Mexico.

³Centro Nacional de Investigación y Desarrollo Tecnológico, Tecnológico Nacional de México, Sonora, Mexico.

Received: August 6, 2019; Accepted: December 17, 2019

Abstract

This paper presents a decentralized model predictive controller for nonlinear systems that considers interaction between control inputs. The controller is based on a centralized robust tube-based nonlinear model predictive controller. The main contribution is a procedure to split the process model into s subsystems in order to construct s robust tube-based controllers ensuring a bounded linearization error. In order to show the applicability and effectiveness of the development, the proposed controller is tested on a coupled-tank system and the results are compared with a centralized nonlinear model predictive controller and a cascade PI controllers scheme.

Keywords: Model predicted control, decentralized control, nonlinear control, robust control.

Resumen

Este artículo presenta un control predictivo descentralizado para sistemas no lineales que considera interacción entre las entradas de control. El controlador se base en un control no lineal predictivo centralizado basado en tubos. La principal contribución es el procedimiento de separar el modelo en s subsistemas para contruir s controladores robustos basados en tubos que aseguren que error de linealización esté acotado. Para demostrar la aplicabilidad y efectividad del desarrollo, el controlador propuesto se prueba en un sistema de tanques acoplados y los resultados se comparan con un control predictivo no lineal centralizado y un esquema de controladores PI en cascada.

Palabras clave: Control predictivo, control descentralizado, control no lineal, control robusto.

1 Introduction

Model Predictive Control (MPC) was introduced as Model Predictive Heuristic Control (Richalet *et al.*, 1978). With great success from its beginnings in industrial applications, Dynamic Matrix Control (DMC) (Cutler & Ramaker, 1979), Generalized Predictive Control (GPC) (Clark *et al.*, 1987; Clark *et al.*, 1987) and Predictive Functional Control (PFC) (Richalet, 1993) were the first linear developments. The space state formulation was proposed later opening the possibility to deal with open-loop stable and unstable systems (Marquis & Broustails, 1988;

Lee *et al.*, 1992; Lee *et al.*, 1994; Morari M. *et al.*, 1994). This MPC representation facilitated the stability analysis (Kwon & Byun, 1989; Rawlings & Musle, 1993; Mayne D. *et al.*, 1993), robustness against parameter uncertainty, noise and bounded disturbances (Bemporad & Morari, 1999), and now, it can be found in the literature MPC developments for specific applications (e.g. a gyroscopic inverted pendulum system (Chu & Chen, 2017), a reverse osmosis unit (Rivas-Perez *et al.*, 2016), a PSA process (Rumbo-Morales *et al.*, 2018)). Nonlinear formulations were also developed (Patwardhan *et al.*, 1990), rendering a nonlinear and possibly non-convex optimization problem, increasing the complexity of the solution (Morari & Lee, 1993).

* Corresponding author. E-mail: jjrumbo@hotmail.com

Tel. 777-564-73-45

<https://doi.org/10.24275/rmiq/Sim778>

issn-e: 2395-8472

Robust MPC formulation is the tube-based model predictive control (tube-based MPC) is another variation of model predictive control, and was applied to linear systems (Langson *et al.*, 2004). This scheme generates tubes that are optimized within the state space. It is guaranteed that the control law maintains the desired controlled variables in the tube, despite model parameter uncertainties. Modifications to this scheme considered bounded disturbances (Mayne *et al.*, 2005) and it was extended to nonlinear systems under additive disturbances (Mayne *et al.*, 2011).

Gonzalez *et al.* (2011) proposed a controller for time-varying systems with additive uncertainty. It is stated that the approach improves the scheme presented by Langson *et al.* (2004), due to a larger generation of the solution feasibility region. As a consequence, a tube-based MPC scheme applied to mobile robots modelled as time-varying systems was presented by Gonzalez *et al.* (2011).

Cannon *et al.* (2009) developed a stochastic tube-based MPC for linear systems with additive and multiplicative uncertainty. Afterwards, a tube-based MPC for nonlinear systems was formulated. This scheme proposes an online system linearization in order to construct tubes along the prediction trajectories guaranteeing robustness against linearization errors (Cannon *et al.*, 2011).

The development of a tube-based MPC scheme for systems with additive uncertainties was presented in Limon *et al.* (2010). These uncertainties are confined to a bounded polyhedral set, corroborating its effectiveness through a set of experimental tests in a four-tank system. In the context of distributed control, MPC has been developed in distributed form called Distributed MPC (DMPC), based on the partition of the system model into several subsystems. From its conception, DMPC was formulated considering only state interaction between subsystems and no interactions between inputs and outputs (Jia & Krogh, 2001; Camponogara *et al.*, 2002). Later works addressed the dynamical relationship between inputs (Venkat *et al.*, 2008) and the entire interaction between the state, inputs and outputs of the system (Vacarini *et al.*, 2009; Sorcía-Vázquez *et al.*, 2015), disturbance rejection (Zheng *et al.*, 2017), or even considering the dynamics of the network as it is the data package dropouts (Zhang *et al.*, 2019).

A novel tube-based distributed MPC was introduced by Trodden & Richards (2010) for multiple dynamically decoupled systems. Distributed control agents exchange plans to achieve a set of coupling constraints. This algorithm presents robustness against persistent disturbances and low susceptibility to communication and computation adverse effects. In this context, a controller was proposed for robotic vehicles in order to avoid obstacles (Trodden & Richards, 2014).

Riverso & Ferrari-Trecate (2012) introduced a tube-based distributed MPC for linear constrained systems. This formulation depends on the availability of a decentralized stabilizing regulator with a two-layer controller for each subsystem. The upper controller receives planned trajectories from neighboring subsystems and the lower controller generates planned trajectories using MPC. The scheme applies the tube notation presented by Langson *et al.* (2004) for achieving, with respect to the coupling, robust stability.

Unlike the papers presented before (Trodden & Richards, 2010; Trodden & Richards, 2014; Riverso & Ferrari-Trecate, 2012), the proposed controller called decentralized robust tube-based model predictive control (DNMPC) is based on the centralized MPC presented in (Cannon *et al.*, 2011). The main advantage of the tube-based MPC is that the nonlinear system model is not used to construct the prediction model as, in some cases, it can be a model of great complexity; instead, the prediction model uses a linear model that is obtained through online linearization at each step time.

The decentralized robust tube-based model predictive control, with the characteristic of online linearizing each nonlinear local model, considers that the system has control input interactions, as it is the interaction type most frequently found in the process industry. Interacting control inputs are sent through a Local Area Network (LAN) to each local subcontroller, where the main assumption is that the controller only introduces one sample-time delay.

The paper has the follow structure: Section 2 presents the background on MPC; Section 3 addresses the development of the decentralized MPC scheme; Section 4 presents the numerical results obtained from applying the centralized MPC, the decentralized MPC and cascade PI scheme to a four-tank process; finally, conclusions are presented in Conclusions.

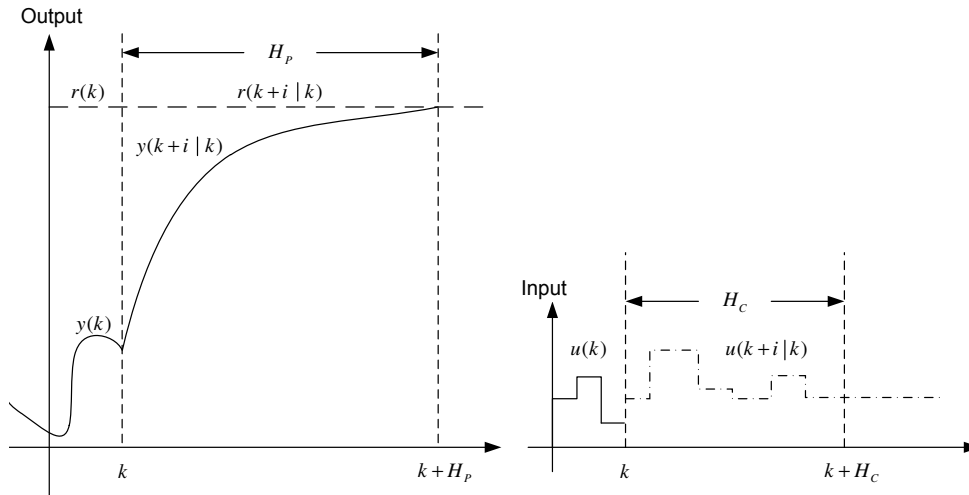


Fig. 1. Model Predictive Control Strategy.

2 Preliminaries of Model Predictive Control

Model Predictive Control (MPC), as it was mentioned in the introduction, was introduced in the late seventies and has developed considerably since then. The term Model Predictive Control does not designate a specific control strategy but rather an ample range of control methods which make explicit use of a model of the process in order to obtain the control signal by minimizing an objective function or a cost function. These design methods lead to controllers which have practically the same structure and present adequate degree of freedom. The main ideas appearing, in greater or lesser degree, in the predictive control family are:

- explicit use of a model to predict the process output at future time instance (horizon);
- calculation of a control sequence minimizing an objective or cost function; and
- receding strategy, so that at each instant the horizon is displaced towards the future, which involves the application of the first control signal of the sequence calculated at each step (Camacho & Bordons, 2007).

MPC presents a series of advantages over other methods, amongst which the following stand out:

- The predictive control is very intuitive, so it

becomes particularly attractive to staff with only a limited knowledge of control.

- It can be used to control a great variety of processes; the multivariable case can easily be dealt with; it intrinsically has compensation for dead times.
- It introduces feed forward control in a natural way to compensate for measurable disturbances.
- The resulting controller is an easy-to-implement control law.
- Its extension to the treatment of constraints is conceptually simple, and these can be systematically included during the design process.
- It is very useful when future references (robotics or batch processes) are known.
- It is a totally open methodology based on certain basic principles which allows for future extensions (Camacho & Bordons, 2007, 2007).

The methodology of all the controllers belonging to the MPC family is characterized by the following strategy, represented in Fig. 1:

1. The future outputs for a determined horizon N , called the prediction horizon, are predicted at each instant t using the process model. These predicted outputs $y(k+i|k)$ (for $i = 1 \dots H_p$) depend on the known values up to instant k (past inputs and outputs) and on the future control

signals $u(k+i|k)$ (for $i = 0 \dots H_C$), which are those to be sent to the system and calculated.

2. The set of future control signals is calculated by optimizing a determined criterion to keep the process as close as possible to the reference trajectory $r(k+i)$ (which can be the setpoint itself or a close approximation of it). This criterion usually takes the form of a quadratic function of the errors between the predicted output signal and the predicted reference trajectory. The control effort is included in the objective function in most cases.
3. The control signal $u(k|k)$ is sent to the process whilst the next control signals calculated are rejected, because at the next sampling instant $y(k+1)$ is already known and step 1 is repeated with this new value and all the sequences are brought up to date. Thus the $u(k+1|k+1)$ is calculated (which in principle will be different from the $u(k+1|k)$ because of the new information available) using the receding horizon concept (Camacho & Bordons, 2007, 2007).

In order to implement this strategy, the basic structure shown in Fig. 2 is used. A model is used to predict the future plant outputs, based on past and current values and on the proposed optimal future control actions. These actions are calculated by the optimizer taking into account the cost function (where the future tracking error is considered) as well as the constraints. The process model plays, in consequence, a decisive role in the controller. The chosen model must be able to capture the process dynamics to precisely predict the future outputs and be simple to

implement and understand. As MPC is not a unique technique but rather a set of different methodologies, there are many types of models used in various formulations (Camacho & Bordons, 2007).

Regarding the robust MPC methodology based on tubes (Cannon *et al.*, 2011), this methodology is based on the construction of ellipses along the prediction trajectory in order to generate bounds on the linearization errors of each linear model.

The construction of a tube for a given predicted trajectory is depicted in Fig. 3. From the referred figure, there is a given predicted trajectory whose initial point is \mathbf{x}_0 . At the point $\mathbf{x}_k^0 + \mathbf{z}_k$, the uncertainty due to the linearization errors is contained within the set $E(\mathbf{V}_k, \beta_k^2)$, as well as the predicted system state \mathbf{x}_k . The next step is to find the set $E(\mathbf{V}_{k+1}, \beta_{k+1}^2)$ for the next predicted state $\mathbf{x}_{k+1}^0 + \mathbf{z}_{k+1}$. This process is repeated until the end of the prediction horizon N . The ellipse generated by the set $E(\mathbf{V}_N, \beta_N^2)$, as a consequence, is contained in the ellipse generated by the terminal set $E(\hat{\mathbf{V}}, 1)$. This terminal is calculated off-line (Buerger, 2013).

The robust MPC based on tubes presents some advantages respect the basic MPC controllers:

- It is a nonlinear control scheme, which considers the complete dynamic of the system.
- This control strategy generate linear models of the process along the predicted trajectory.
- It is a robust control technique, which generate bounds around the linearization errors.
- The process can be controlled at any operation point without having to make modifications.

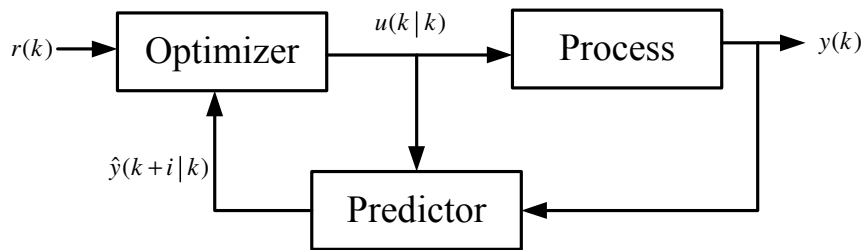


Fig. 2. Basic structure of Model Predictive Controller.

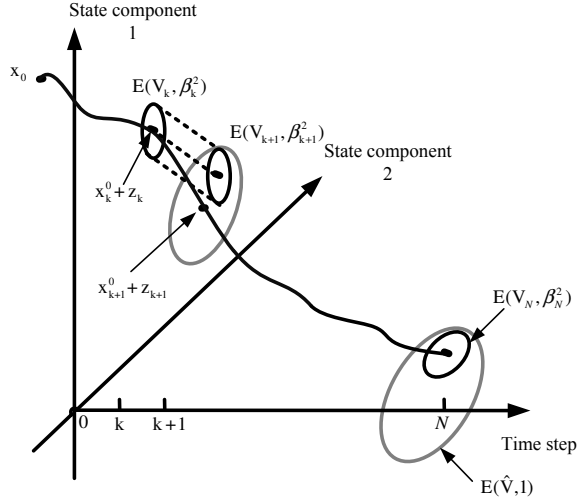


Fig. 3. Predicted state trajectory contained in a tube (Buerger, 2013).

On the other hand, the robust MPC also presents some disadvantages:

- Linear matrix inequalities (LMI) are involved that must be resolved online.
- The solution of the optimization problem requires high computational resources.
- It is highly complex to implement the controller in real time, because it requires solving a second order cone program.

The details of the centralized robust MPC are shown in the Appendix. The following section presents the development of the decentralized robust model predictive control.

3 Nonlinear decentralized robust model predictive control

The present section addresses the nonlinear decentralized robust model predictive control (DNMPC). This control scheme is an extension of the centralized robust tube-based model predictive control (Cannon et al., 2011).

3.1 Nonlinear decentralized robust model predictive control

The development of the decentralized robust model predictive control considers the following nonlinear

systems general definition conformed by s subsystems with interaction between control inputs

$$\mathbf{x}_{i|k+1} = f_i(\mathbf{x}_{i|k}, \mathbf{u}_{1|k}, \dots, \mathbf{u}_{s|k}), \quad (1)$$

where $\mathbf{x}_{i|k} \in \mathbb{R}^{n_i}$ and $\mathbf{u}_{i|k} \in \mathbb{R}^{m_i}$ are the state and the control signal vectors for each subsystem, respectively. In (1), f_i is continuous and differentiable for all $(\mathbf{x}_i, \mathbf{u}_i)$ in an operating region, and $f_i(0, 0) = 0$ with $i = 1, \dots, s$.

The design is based on a local optimal regulation problem for each subsystem with respect a local quadratic cost function

$$J_i = \sum_{k=0}^{\infty} (\|\mathbf{x}_{i|k}\|_{\mathbf{Q}_i}^2 + \|\mathbf{u}_{i|k}\|_{\mathbf{R}_i}^2), \quad (2)$$

subject to decentralized lineal restrictions of the form

$$\mathbf{F}_i \mathbf{x}_{i|k} + \mathbf{G}_i \mathbf{u}_{i|k} \leq \mathbf{h}_i, \quad k = 0, 1, \dots, \quad (3)$$

where $\mathbf{F}_i \in \mathbb{R}^{n_{u_i} \times n_i}$, $\mathbf{G}_i \in \mathbb{R}^{n_{u_i} \times m_i}$. It is assumed that the state of each subsystem \mathbf{x}_i is measured at each time step k .

For each local subsystem, state and control input trajectories from time instant k to the horizon N are stipulated as well as the interacting control input predictions over the $k - 1$ time instant. These considerations are defined as $\{\mathbf{x}_{i|k+l|k}^0, \mathbf{u}_{i|k+l|k}^0, l = 0, \dots, N - 1\}$ in the following expression, in concordance to the model (1)

$$\mathbf{x}_{i|(k+l+1)|k}^0 = f(\mathbf{x}_{i|(k+l)|k}^0, \mathbf{u}_{i|(k+l)|k}^0, \mathbf{u}_{j|(k+l)|k-1}^0, \dots, \mathbf{u}_{s|(k+l)|k-1}^0),$$

with $\mathbf{x}_{i|k|k}^0 = \mathbf{x}_{i|k}$ representing the measured current state for each local subsystem and $j = 1, \dots, s, j \neq i$.

The subsystem state and control input are redefined as function of the predicted state and input, therefore

$$\begin{aligned} \mathbf{x}_{i|k+l|k} &= \mathbf{x}_{i|k+l|k}^0 + \mathbf{x}_{i|k+l|k}^\delta, \\ \mathbf{u}_{i|k+l|k} &= \mathbf{u}_{i|k+l|k}^0 + \mathbf{u}_{i|k+l|k}^\delta, \end{aligned} \quad (4)$$

for $l = 1, \dots, N - 1$ with $\mathbf{x}_{i|k+l|k}^\delta = 0$. $\mathbf{u}_{i|k+l|k}^\delta$ is parametrized as the sum of a decentralized control law and a feedforward term \mathbf{v}_i ,

$$\mathbf{u}_{i|k+l|k}^\delta = \mathbf{K}_{i|k+l|k} \mathbf{x}_{i|k+l|k}^\delta + \mathbf{v}_{i|k+l|k}. \quad (5)$$

In order to synthesize the DNMPC scheme a decentralized linear time-variant model is used, with the following general form

$$\mathbf{x}_{i|k+l+1|k}^\delta = \Phi_{i|k+l|k} \mathbf{x}_{i|k+l|k}^\delta + \mathbf{B}_{i|k+l|k} \mathbf{v}_{i|k+l|k} + \mathbf{w}_{i|k+l|k}, \quad (6)$$

Let us point out that this model is derived from the linearization of the nonlinear model (1) around $\mathbf{x}_{ik+l|k}^0, \mathbf{u}_{ik+l|k}^0$

$$\Phi_{ik+l|k} = \mathbf{A}_{ik+l|k} + \mathbf{B}_{ik+l|k} \mathbf{K}_{ik+l|k};$$

$$\mathbf{A}_{ik+l|k} = \left. \frac{\partial f}{\partial \mathbf{x}_{ik}} \right|_{\mathbf{x}_{ik+l|k}^0, \mathbf{u}_{ik+l|k}^0},$$

$$\mathbf{B}_{ik+l|k} = \left. \frac{\partial f}{\partial \mathbf{u}_{ik}} \right|_{\mathbf{x}_{ik+l|k}^0, \mathbf{u}_{ik+l|k}^0},$$

with $\mathbf{w}_{ik+l|k}$ representing the linearization error for each subsystem. Predictions for $l \geq N$ are determined from the linearization error of (1), around the target setpoint $(\mathbf{x}_{ik}, \mathbf{u}_{ik}) = (0, 0)$ and a decentralized fixed feedback control law $\hat{\mathbf{K}}_i \mathbf{x}_{ik}$

$$\mathbf{x}_{ik+l+1|k} = \hat{\Phi}_i \mathbf{x}_{ik+l|k} + \hat{\mathbf{w}}_{ik+l|k}; \quad (7)$$

$$\mathbf{u}_{ik+l|k} = \hat{\mathbf{K}}_i \mathbf{x}_{ik+l|k}, \quad (8)$$

for $l = N, N + 1, \dots$, where $\hat{\Phi}_i = \hat{\mathbf{A}}_i + \hat{\mathbf{B}}_i \hat{\mathbf{K}}_i$, with $\hat{\mathbf{A}}_i = \left. \frac{\partial f_i}{\partial \mathbf{x}_{ik}} \right|_{(0,0)}$, $\hat{\mathbf{B}}_i = \left. \frac{\partial f_i}{\partial \mathbf{u}_{ik}} \right|_{(0,0)}$.

A boundary condition from the linearization errors \mathbf{w}_i and $\hat{\mathbf{w}}_i$ of each subsystem can be used to bound the predicted cost and to determine a robust feasible constraint set. Since f_i is continuous and differentiable, exists a convex set $\Omega_i \subset \mathbb{R}^{n_i \times (n_i + m_i)}$ such that $\mathbf{w}_{ik} \in \Omega_i \left[\begin{matrix} \mathbf{x}_{ik}^\delta & \mathbf{u}_{ik}^\delta \\ \mathbf{0} & \mathbf{0} \end{matrix} \right]^\top$. It is assumed that Ω_i is polytopic with vertices $\left[\begin{matrix} \mathbf{C}_j^i & \mathbf{D}_j^i \end{matrix} \right], j = 1, \dots, p$, so

$$\mathbf{w}_{ik} \in \text{Co} \left\{ \mathbf{C}_j^i \mathbf{x}_{ik}^\delta + \mathbf{D}_j^i \mathbf{u}_{ik}^\delta, j = 1, \dots, p \right\}. \quad (9)$$

In a similar way, the errors $\hat{\mathbf{w}}_{ik+l|k}$ of the linear dynamic approximation (7) with $l \geq N$, will reside within the convex set

$$\hat{\mathbf{w}}_{ik} \in \text{Co} \left\{ \hat{\mathbf{C}}_j^i \mathbf{x}_{ik} + \hat{\mathbf{D}}_j^i \mathbf{u}_{ik}, j = 1, \dots, p \right\}. \quad (10)$$

In order to achieve the linearization error boundary on the predicted trajectories of each subsystem, a tube is constructed containing the arised predicted state component generated from the linearization errors. The tube is used to compute local bounds on the cost and constraints in the DN MPC optimization for each subsystem.

Prediction $\mathbf{x}_{ik+l|k}^\delta$ is divided for the local subsystem in a nominal component $\mathbf{z}_{ik+l|k}$ and a component $\mathbf{e}_{ik+l|k}$, depending uniquely on the linearization error $\mathbf{w}_{ik+l|k}$:

$$\mathbf{x}_{ik+l|k}^\delta = \mathbf{z}_{ik+l|k} + \mathbf{e}_{ik+l|k} \quad (11a)$$

$$\mathbf{z}_{ik+l+1|k} = \Phi_{ik+l|k} \mathbf{z}_{ik+l|k} + \mathbf{B}_{ik+l|k} \mathbf{v}_{ik+l|k} \quad (11b)$$

$$\mathbf{e}_{ik+l+1|k} = \Phi_{ik+l|k} \mathbf{e}_{ik+l|k} + \mathbf{w}_{ik+l|k}, \quad (11c)$$

with $\mathbf{z}_{ik|k} = \mathbf{e}_{ik|k} = 0$.

3.2 Construction of the decentralized tubes with fixed and variable cross sections

A fundamental part of the DN MPC scheme is to generate bounds around the linearization error component $\mathbf{e}_{ik+l+1|k}$ and the state prediction $\mathbf{x}_{ik+l|k}$ of each subsystem. These boundaries are ellipses with fixed or variable cross sections

$$\mathbf{e}_{ik+l|k} \in \mathcal{E}(\mathbf{V}_{ik+l|k}, \beta_{ik+l|k}^2), l = 1, \dots, N \quad (12a)$$

$$\mathbf{x}_{ik+l|k} \in \mathcal{E}(\hat{\mathbf{V}}_i, 1), l \geq N, \quad (12b)$$

where $\mathcal{E}(\mathbf{P}_i, \rho_i^2)$, for $\mathbf{P}_i > 0$, denotes the ellipsoidal set $\mathcal{E}(\mathbf{P}_i, \rho_i^2) = \{ \mathbf{x}_i : \mathbf{x}_i^\top \mathbf{P}_i \mathbf{x}_i \leq \rho_i^2 \}$, for each subsystem. From (12b), $\mathcal{E}(\hat{\mathbf{V}}_i, 1)$ is a local subsystem restriction terminal set, which is invariant under (7) and (8), therefore, it is required

$$\hat{\Phi}_i \mathbf{x}_i + \hat{\mathbf{w}}_i \in \mathcal{E}(\hat{\mathbf{V}}_i, 1), \forall \hat{\mathbf{w}}_i \in \text{Co} \left\{ (\hat{\mathbf{C}}_j^i + \hat{\mathbf{D}}_j^i \hat{\mathbf{K}}_i) \mathbf{x}_i \right\}, \quad (13)$$

$$\forall \mathbf{x}_i \in \mathcal{E}(\hat{\mathbf{V}}_i, 1).$$

It is also required, for $\mathcal{E}(\hat{\mathbf{V}}_i, 1)$, to be feasible with respect to (3) in order to satisfy the input/state restrictions over an infinite prediction horizon. This is accomplished if

$$(\mathbf{F}_i + \mathbf{G}_i \hat{\mathbf{K}}_i) \mathbf{x}_i \leq \mathbf{h}_i, \forall \mathbf{x}_i \in \mathcal{E}(\hat{\mathbf{V}}_i, 1). \quad (14)$$

In order to obtain the matrices $\hat{\mathbf{K}}_i$ and $\hat{\mathbf{V}}_i$ for each subcontroller, a semidefinite program (SDP) is solved off-line to maximize the local terminal set $\mathcal{E}(\hat{\mathbf{V}}_i, 1)$ subject to (13) and (14). Thus, being $\hat{\mathbf{S}}_i, \hat{\mathbf{Y}}_i$ the problem solution:

$$\begin{aligned} & \max \det(\hat{\mathbf{S}}_i) \\ & \hat{\mathbf{S}}_i, \hat{\mathbf{Y}}_i \\ & \text{s. t.} \\ & \left[\begin{array}{cc} \hat{\mathbf{S}}_i & (\hat{\mathbf{A}}_i + \hat{\mathbf{C}}_j^i) \hat{\mathbf{S}}_i + (\hat{\mathbf{B}}_i + \hat{\mathbf{D}}_j^i) \hat{\mathbf{Y}}_i \\ * & \hat{\mathbf{S}}_i \end{array} \right] \geq 0, j = i, \dots, p \\ & \left[\begin{array}{cc} \mathbf{h}_{iq}^2 & \mathbf{F}_{iq} \hat{\mathbf{S}}_i + \mathbf{G}_{iq} \hat{\mathbf{Y}}_i \\ * & \hat{\mathbf{S}}_i \end{array} \right] \geq 0, q = 1, \dots, n_c, \end{aligned} \quad (15)$$

the volume of $\mathcal{E}(\hat{\mathbf{V}}_i, 1)$ is maximized with $\hat{\mathbf{V}}_i = \hat{\mathbf{S}}_i^{-1}$ and $\hat{\mathbf{K}}_i = \hat{\mathbf{Y}}_i \hat{\mathbf{S}}_i^{-1}$, where $\hat{\mathbf{V}}_i$ is the local ellipse generator set and $\hat{\mathbf{K}}_i$ is the local feedback gain.

With the previously mentioned in mind, two kind of tubes can be constructed from the gain $\hat{\mathbf{K}}_i$ and the set $\hat{\mathbf{V}}_i$: (i) fixed cross section tubes and (ii) variable

cross section tubes. Gains based on variable cross section tubes can be computed by solving a local SDP:

$$\begin{aligned} & \max_{\hat{\mathbf{S}}_i, \hat{\mathbf{Y}}_i, \gamma_i} \gamma_i \\ & \text{s. t.} \\ & \mathbf{S}_i \geq \gamma_i \mathbf{I}_i \begin{bmatrix} \mathbf{S}_i & (\mathbf{A}_{ik+l+1|k} + \mathbf{C}_j^i) \mathbf{S}_i + (\mathbf{B}_{ik+l+1|k} + \mathbf{D}_j^i) \mathbf{Y}_i \\ * & \mathbf{V}_{ik+l+1|k}^{-1} \end{bmatrix} \geq 0, \\ & j = 1, \dots, p, \end{aligned} \quad (16)$$

and, finally, by defining $\mathbf{V}_{ik+l|k} = \mathbf{S}_i^{-1}$, $\mathbf{K}_{ik+l|k} = \mathbf{Y}_i \mathbf{S}_i^{-1}$, variable cross section tubes are obtained. Fixed cross section tubes can be computed by solving the SDP (15) with $\mathbf{V}_{ik+l|k} = \hat{\mathbf{V}}_i$, $\mathbf{K}_{ik+l|k} = \hat{\mathbf{K}}_i$.

3.3 Decentralized cost function

A local cost function for each DN MPC subcontroller is given by:

$$\begin{aligned} J_i(\mathbf{x}_{ik}, \mathbf{u}_{ik}) = & \sum_{k=0}^{N-1} \left(\|x_{ik+l|k}\|_{\mathbf{Q}_i}^2 + \|u_{ik+l|k}\|_{\mathbf{R}_i}^2 \right) \\ & + \|x_{ik+N|k}\|_{\mathbf{P}_i}^2, \end{aligned} \quad (17)$$

where \mathbf{P}_i is a local weighting matrix optimized off-line by solving the SDP

$$\begin{aligned} & \min_{\mathbf{P}_i} \text{tr}(\mathbf{P}_i) \\ & \text{s. t.} \\ & \mathbf{P}_i - (\hat{\Phi}_i + \hat{\mathbf{C}}_j^i + \hat{\mathbf{D}}_j^i \hat{\mathbf{K}}_i)^\top \mathbf{P}_i (\hat{\Phi}_i + \hat{\mathbf{C}}_j^i + \hat{\mathbf{D}}_j^i \hat{\mathbf{K}}_i) \\ & \quad \geq \mathbf{Q}_i + \hat{\mathbf{K}}_i^\top \mathbf{R}_i \hat{\mathbf{K}}_i, \\ & j = 1, \dots, p, \end{aligned} \quad (18)$$

Each cost function term from (17) is individually represented as $J_{ix,l}$, $J_{iu,l}$, for $l = 0, \dots, N-1$, and $J_{ix,N}$

$$J_{ix,l} = \left\| x_{ik+l|k}^0 + z_{ik+l|k} \right\|_{\mathbf{Q}_i} + \beta_{ik+l|k} \left\| \mathbf{V}_{ik+l|k}^{-1/2} \right\|_{\mathbf{Q}_i} \quad (19a)$$

$$J_{iu,l} = \left\| u_{ik+l|k}^0 + \mathbf{K}_{ik+l|k} z_{ik+l|k} + v_{ik+l|k} \right\|_{\mathbf{R}_i} \quad (19b)$$

$$+ \beta_{ik+l|k} \left\| \mathbf{K}_{ik+l|k} \mathbf{V}_{ik+l|k}^{-1/2} \right\|_{\mathbf{R}_i} \quad (19c)$$

$$J_{ix,N} = \left\| x_{ik+N|k}^0 + z_{ik+N|k} \right\|_{\mathbf{P}_i} + \beta_{ik+N|k} \left\| \hat{\mathbf{V}}_i^{-1/2} \right\|_{\mathbf{P}_i} \quad (19d)$$

Proposition 3.1 Consider a decentralized nonlinear system (1), a terminal set and a set of gains varying along the prediction trajectory, obtained by solving (15-16), that generate fixed or variable cross section tubes. Considering local cost functions of the form (17) a Decentralized Nonlinear Model Predictive

Control (DN MPC) can be obtained if the following conical problem is feasible:

$$(\mathbf{v}_{ik}^*, \beta_{ik}^*) = \min_{\mathbf{v}_{ik}, \beta_{ik}} \sum_{l=0}^{N-1} (J_{ix,l}^2 + J_{iu,l}^2) + J_{ix,N}^2 \quad (20a)$$

$$\text{s. t.} \quad \mathbf{z}_{ik+l+1|k} = \Phi_{ik+l|k} \mathbf{z}_{ik+l|k} + \mathbf{B}_{ik+l|k} \mathbf{v}_{ik+l|k} \quad (20b)$$

$$\beta_{ik+l+1|k} \geq \lambda_{l,j} \beta_{ik+l|k} + \left\| (\mathbf{C}_j^i + \mathbf{D}_j^i \mathbf{K}_{ik+l|k}) \mathbf{z}_{ik+l|k} + \mathbf{D}_j^i v_{ik+l|k} \right\| \quad (20c)$$

$$J_{ix,l} \geq \left\| x_{ik+l|k}^0 + z_{ik+l|k} \right\|_{\mathbf{Q}_i} + \beta_{ik+l|k} \left\| \mathbf{V}_{ik+l|k}^{-1/2} \right\|_{\mathbf{Q}_i} \quad (20d)$$

$$\begin{aligned} J_{iu,l} \geq & \left\| u_{ik+l|k}^0 + \mathbf{K}_{ik+l|k} z_{ik+l|k} + v_{ik+l|k} \right\|_{\mathbf{R}_i} \\ & + \beta_{ik+l|k} \left\| \mathbf{K}_{ik+l|k} \mathbf{V}_{ik+l|k}^{-1/2} \right\|_{\mathbf{R}_i} \end{aligned} \quad (20e)$$

$$\begin{aligned} \mathbf{h}_{iq} \geq & (\mathbf{F}_{iq} x_{ik+l|k}^0 + \mathbf{G}_{iq} u_{ik+l|k}^0) + (\mathbf{F}_{iq} + \mathbf{G}_{iq} \mathbf{K}_{ik+l|k}) \mathbf{z}_{ik+l|k} \\ & + \mathbf{G}_{iq} v_{ik+l|k} + \beta_{ik+l|k} \left\| (\mathbf{F}_{iq} + \mathbf{G}_{iq} \mathbf{K}_{ik+l|k}) \right\|_{\mathbf{V}_{ik+l|k}^{-1}} \end{aligned} \quad (20f)$$

$$\text{for } l = 1, \dots, N-1, y \quad (20g)$$

$$\mathbf{z}_{ik|k} = 0 \quad (20h)$$

$$\beta_{ik|k} = 0 \quad (20i)$$

$$1 \geq \left\| x_{ik+N|k}^0 + z_{ik+N|k} \right\|_{\hat{\mathbf{V}}} + \beta_{ik+N|k} \quad (20j)$$

where $\lambda_{l,j} = 1$ if a variable cross section tubes are used or $\lambda_{l,j} = \left\| \Phi_{ik+l|k} \hat{\mathbf{V}}_i^{-1/2} \right\|_{\hat{\mathbf{V}}_i} + \left\| (\mathbf{C}_j^i + \mathbf{D}_j^i \hat{\mathbf{K}}_i) \hat{\mathbf{V}}_i^{-1/2} \right\|_{\hat{\mathbf{V}}_i}$ if a fixed cross section tubes are used.

From Proposition 3.1, Algorithm 1 is established. This algorithm describes the steps to follow in order to apply the DN MPC scheme.

4 Four-tank system

The four-tank process is a multivariable plant of interconnected tanks, used to validate the proposed DN MPC scheme. The process has two direct current pumps and two three-way valves that distribute the flow generated by the pumps to the tanks. The process model representing its dynamics can be partitioned into two subsystems. Depending on the partition done on the process model, this process can exhibit input or state interaction (Johansson, 2000).

The Fig. 4 shows the quadruple-tank schematic diagram. The output flow of Tank 2 feeds Tank 1 and the output flow of the Tank 3 feeds Tank 4.

Algorithm 1 (DNMPC)

- 1: *Offline*: Compute $\hat{\mathbf{V}}_i, \hat{\mathbf{K}}_i$ by solving (15) that define the terminal set and control law. Solve (18) to compute the terminal weight matrix \mathbf{P}_i .
- 2: *Online*: set $k = 0$:
- 3: Find initial conditions $\mathbf{u}_{i0}^0, \mathbf{x}_{i0}^0$ using the interacting input prediction $\underline{\mathbf{u}}_{j0|k-1}^0$.
- 4: Initialize $iter=1$. Given \mathbf{u}_{ik}^0 , calculate \mathbf{x}_{ik}^0 that satisfies (1) with $\mathbf{x}_{ik|k}^0 = \mathbf{x}_{ik}$.
- 5: Linearize the model (1) around $\mathbf{u}_{ik}^0, \mathbf{x}_{ik}^0$ without considering the inputs to determine $\mathbf{A}_{ik+l|k}, \mathbf{B}_{ik+l|k}$ for $l = 0, \dots, N-1$.
- 6: **If** a variable cross section tubes are used, calculate $\mathbf{V}_{ik+l|k}$ and $\mathbf{K}_{ik+l|k}$ by solving (16) for $l = N-1, \dots, 0$ with $\mathbf{x}_{ik|k}^\delta = 0$,
- 7: **Else**, assign $\mathbf{V}_{ik+l|k} = \hat{\mathbf{V}}_i, \mathbf{K}_{ik+l|k} = \hat{\mathbf{K}}_i$ for fixed cross section tubes.
- 8: Solve (20) to determine \mathbf{v}_{ik}^* .
- 9: Determine $\mathbf{x}_{ik}, \mathbf{u}_{ik}$ satisfying (1), (4), (5) with $\mathbf{v}_{ik} = \mathbf{v}_{ik}^*$ by means of: (a) the use of (4) and (5) to calculate $\mathbf{u}_{ik+l|k}$ given $\mathbf{x}_{ik+l|k}, \mathbf{v}_{ik+l|k}, \mathbf{x}_{ik+l|k}^0, \mathbf{u}_{ik+l|k}^0$; (b) the use of (1) to calculate $\mathbf{x}_{ik+l|k}$; for $i = 0, \dots, N-1$ con $\mathbf{x}_{k|k}^\delta = 0$.
- 10: **If** $iter < Maxiters$ and $\|\mathbf{v}_k^*\| \geq tolerance$, assign $\mathbf{x}_k^0 = \mathbf{x}_k, \mathbf{u}_k^0 = \mathbf{u}_k, iter = iter + 1$ and return to step 5.
- 11: **Else**, assign

$$\mathbf{u}_{ik+1}^0 = \left\{ \mathbf{u}_{ik+1|k}, \dots, \mathbf{u}_{ik+N-1|k}, \hat{\mathbf{K}}\mathbf{x}_{ik+N|k+1} \right\}$$

and implement $\mathbf{u}_k = \mathbf{u}_{k|k} + \mathbf{v}_{k|k}^*$.

- 12: Acquire through the LAN the predicted control inputs trajectories of the interacting subsystems $\underline{\mathbf{u}}_{j0|k-1}^0$.
- 13: Increment the index $k = k + 1$ and return to step 3.

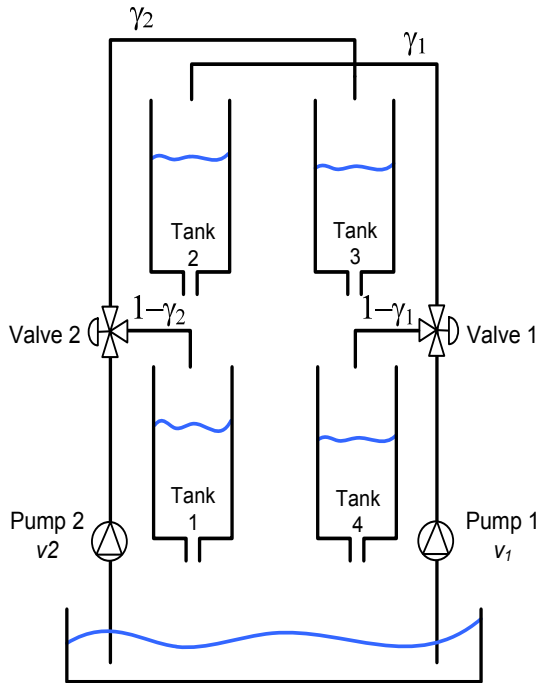


Fig. 4. Four tanks system scheme.

Regarding the output flow of the pumps, the flow of the Pump 2 feeds Tank 1 and Tank 3 through valve 2; the flow of the Pump 1 feeds Tank 2 and Tank 4 through valve 1. Considering the structure of the tank system, the system partitioning can be done in two ways: (i) considering Tanks 1 and 2 as Subsystem 1 and Tanks 3 and 4 as Subsystem 2, obtaining input interactions but not states interactions; and (ii) considering Tanks 1 and 3 as Subsystem 1 and Tanks 2 and 4 as Subsystem 2, obtaining interaction between states but not between inputs. For the application of the DNMPC scheme, the first option was selected.

4.1 Four-tank system model

The nonlinear model of the four-tank system is computed from the interaction between the input and output flows. This model is given by the following differential equations:

$$\dot{h}_1 = -\frac{a_1}{A_1} \sqrt{2gh_1} + \frac{a_2}{A_1} \sqrt{2gh_2} + \frac{(1-\gamma_2)k_2}{A_1} v_2 \quad (21)$$

$$\begin{aligned} \dot{h}_2 &= -\frac{a_2}{A_2} \sqrt{2gh_2} + \frac{\gamma_1 k_1}{A_2} v_1 \\ \dot{h}_3 &= -\frac{a_3}{A_3} \sqrt{2gh_3} + \frac{\gamma_2 k_2}{A_3} v_2 \\ \dot{h}_4 &= -\frac{a_4}{A_4} \sqrt{2gh_4} + \frac{a_3}{A_4} \sqrt{2gh_3} + \frac{(1-\gamma_1)k_1}{A_4} v_1, \end{aligned}$$

where $\dot{\mathbf{x}} = [\dot{h}_1, \dot{h}_2, \dot{h}_3, \dot{h}_4]^T$, $\mathbf{x} = [h_1, h_2, h_3, h_4]^T$, $\mathbf{u} = [v_1, v_2]^T$, h_i the level of tank i , v_i the voltage applied to the pump i and the rest of the parameter values are shown in Table 1 defining the physical geometry of the system.

As it was described at the beginning of this section, the model (21) is partitioned as follows: Subsystem 1 is conformed by the equations of Tanks 1 and 2

$$\begin{aligned} \dot{h}_1 &= -\frac{a_1}{A_1} \sqrt{2gh_1} + \frac{a_2}{A_1} \sqrt{2gh_2} \\ &\quad + \frac{(1-\gamma_2)k_2}{A_1} v_2; \\ \dot{h}_2 &= -\frac{a_2}{A_2} \sqrt{2gh_2} + \frac{\gamma_1 k_1}{A_2} v_1; \end{aligned} \tag{22}$$

and Subsystem 2 is conformed by the equations of Tanks 3 and 4

$$\begin{aligned} \dot{h}_3 &= -\frac{a_3}{A_3} \sqrt{2gh_3} + \frac{\gamma_2 k_2}{A_3} v_2; \\ \dot{h}_4 &= -\frac{a_4}{A_4} \sqrt{2gh_4} + \frac{a_3}{A_4} \sqrt{2gh_3} \\ &\quad + \frac{(1-\gamma_1)k_1}{A_4} v_1. \end{aligned} \tag{23}$$

With the partitioned system, Subsystem 1 has the state vector $\mathbf{x}_1 = [h_1, h_2]$ and Subsystem 2 has the state vector $\mathbf{x}_2 = [h_3, h_4]$. The main control input of Subsystem 1 is $\mathbf{u}_1 = v_1$, which corresponds to the

pump 1 shared with Subsystem 2 through valve 1. In a similar way, the main control input of Subsystem 2 is $\mathbf{u}_2 = v_2$ (pump 2) shared with Subsystem 1 through valve 2.

4.2 Numerical results

4.2.1 Centralized controller application

In order to apply the centralized controller to the plant, a discrete-time model of the four-tank process with the state $\mathbf{x}_k = [h_1(kT), h_2(kT), h_3(kT), h_4(kT)]^T$ and sampling time $T = 3$ s is computed online, with the initial condition $\mathbf{x}_0 = [5, 2, 2, 6]^T$ and $N = 15$. For the setpoints $\mathbf{x}_r = [10.8, 4.9, 3.8, 10.1]^T$, $\forall t \in [0, 75]$ and $\mathbf{x}_r = [15, 6.7, 5.7, 14.4]^T$, $\forall t \in [75, 150]$, and weight matrices $\mathbf{Q} = 20 \times \mathbf{I}$, $\mathbf{R} = 0.1 \times \mathbf{I}$, with \mathbf{I} defined as an identity matrix of compatible dimensions. The terminal set parameters $\hat{\mathbf{K}}$ and $\hat{\mathbf{V}}$ are computed off-line subject to bounds $|\mathbf{x} - \mathbf{x}_r| \leq 2 \times [1, 1, 1, 1]^T$. The pump control signals have the following constraints

$$\begin{bmatrix} 0 \\ 0 \end{bmatrix} \leq \mathbf{u} \leq \begin{bmatrix} 10 \\ 10 \end{bmatrix}$$

where $\mathbf{u} = [v_1, v_2]^T$.

In Fig. 5, left column, the evolution of tank levels with centralized MPC and variable gain tubes is shown, and the right column shows the evolution tank levels with centralized MPC with fixed gain tubes. Top sub-plots present the evolution of levels in the (h_1, h_2) plane, and bottom sub-plots the evolution of levels in the (h_3, h_4) plane. From the referred figure, the tank levels reach a steady state within the terminal set $\hat{\mathbf{V}}$, but it can not be plotted easily as it is in \mathbb{R}^4 .

The Fig. 6 shows the tank levels evolution using the centralized MPC with fixed gains and cross section tubes. The tank levels converge successfully to desired

Table 1: Quadruple-Tank parameters

Parameter	Variable	Value	Units
Pump gains	(k_1, k_2)	(3.35, 3.33)	$[\text{cm}^3/\text{Vs}]$
3-way valves	(γ_1, γ_2)	(0.6, 0.7)	
Area Tanks 1 and 2	(A_1, A_2)	28	$[\text{cm}^2]$
Area Tanks 3 and Discharge constant of Tanks 1 and 2	(a_1, a_2)	0.071	$[\text{cm}^2]$
Discharge constant of Tanks 3 and 4	(a_3, a_4)	0.057	$[\text{cm}^2]$
Level sensor gains	k_c	0.5	$[\text{V}/\text{cm}]$
Gravitational constant	g	981	$[\text{cm}/\text{s}^2]$

reference. Tanks 2 and 3 present an overshoot and Tanks 1 and 4 have a smooth convergence due to the fact that the output flow of the pumps enter directly to the Tanks 2 and 3. Bottom sub-plot presents the control signals applied to the pumps, with values within the defined limits.

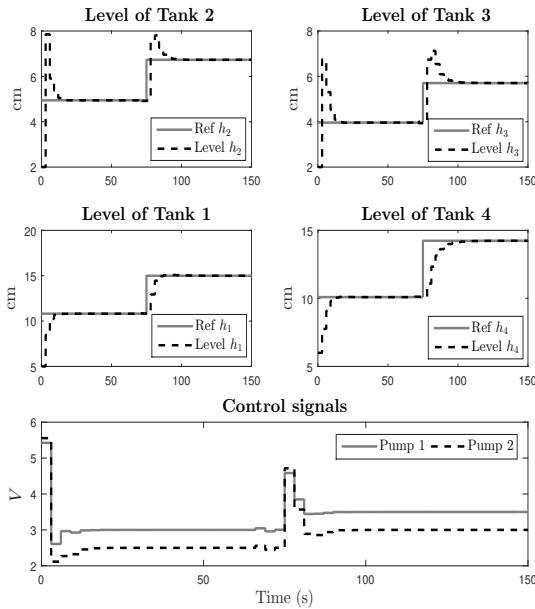


Fig. 6. Tank levels and control signals for the centralized controller with fixed gains.

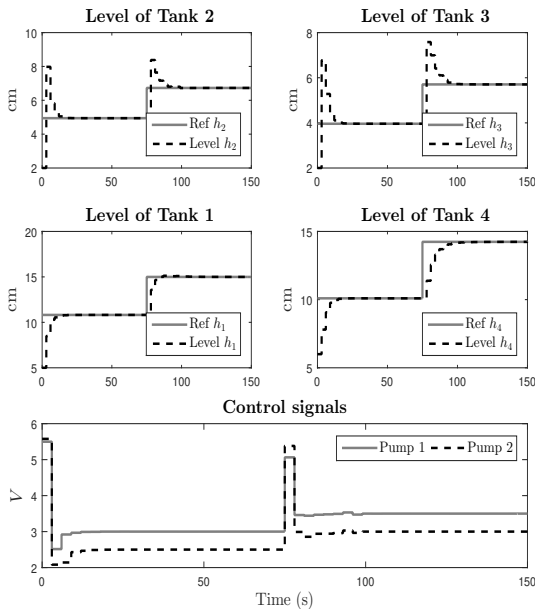


Fig. 7. Tank levels and control signal for the centralized controller with variable gains.

The Fig. 7 shows the results obtained when the centralized MPC with variable gains and cross section tubes is used. As in the results obtained when fixed gain and cross section tubes were applied, tank levels converge to the desired reference. It can be observed that the level evolution is similar with respect to the results obtained with the fixed gains and cross section tubes. The pump control signals present slight differences compared with the results shown in Fig. 6.

4.2.2 Decentralized controller application

Addressing the application of the DN MPC scheme, two discrete models of the tank systems with the states $\mathbf{x}_{1k} = [h_1(kT), h_2(kT)]^T$, $\mathbf{x}_{2k} = [h_3(kT), h_4(kT)]^T$ and sampling time $T = 3$ s are computed online, with the initial conditions $\mathbf{x}_1^0 = [5, 2]^T$, $\mathbf{x}_2^0 = [2, 6]^T$ and $N = 15$. The initial conditions and the prediction horizon are similar to those used in the centralized scheme. The setpoints are divided for each subsystem as $\mathbf{x}_{1r} = [10.8, 4.9]^T$, $\mathbf{x}_{2r} = [3.8, 10.1]^T$, $\forall t \in [0, 75]$ and $\mathbf{x}_{1r} = [15, 6.7]^T$, $\mathbf{x}_{2r} = [5.7, 14.4]^T$, $\forall t \in [75, 150]$, and weight matrices $\mathbf{Q}_1 = \mathbf{Q}_2 = 0.1 \times \mathbf{I}$, $\mathbf{R}_1 = \mathbf{R}_2 = 1$.

Fig. 8 shows the evolution of tank levels with the decentralized MPC. The left column presents the results obtained with variable gain tubes and the second column presents the results obtained with fixed gain tubes. In both cases, levels reach a steady state within the terminal sets. Each setpoint \mathbf{x}_{ir} generate its own terminal set and, unlike the previous result, it is possible to plot the terminal sets because each subsystem belongs to \mathbb{R}^2 .

Fig. 9 presents the evolution of tank levels for a single step time k . As it is observed, the predicted trajectory (grey line) is in the tube generated by the ellipses (solid black) and the initial trajectory \mathbf{x}_{i0}^0 is represented by the dashed black line. Both trajectories converge to the terminal set (dashed ellipse). The left column of the figure shows the results obtained with variable gain tubes and the right column shows the results obtained with fixed gain tubes. The variable gain tubes generate ellipses with a larger cross section than the ellipses generated by the fixed gain tubes, this represents a better disturbance rejection, which allows for larger perturbations \mathbf{x}_i^δ , \mathbf{u}_i^δ for each subsystem.

Fig. 10 presents tank levels with the decentralized MPC using fixed gain tubes. The tank levels converge to the desired setpoint and, in comparison with the results obtained with the centralized controller, Tanks 2 and 3 have smaller overshoots. In the same way, Fig. 11 presents the results with the decentralized MPC using variable gain tubes. As in the results obtained

with fixed gains, the tank levels converge to desired setpoint. Comparing the results of the Fig. 10 and Fig. 11, the behavior of the levels is similar, only the pump control signals present slight differences, which can be observed at the bottom of the figures.

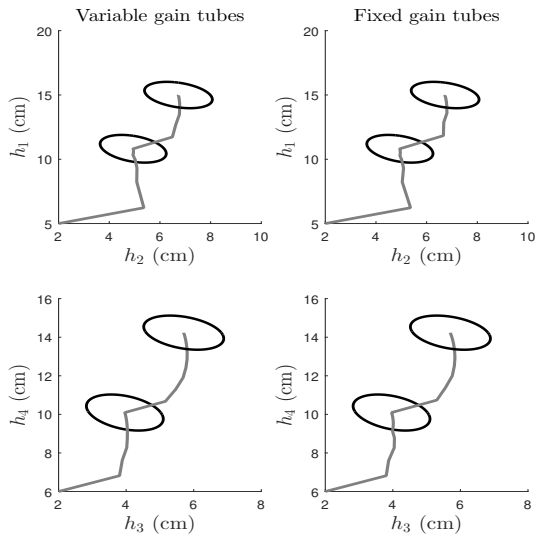


Fig. 8. Evolution of the tank levels and their convergence to the terminal sets with the decentralized controller.

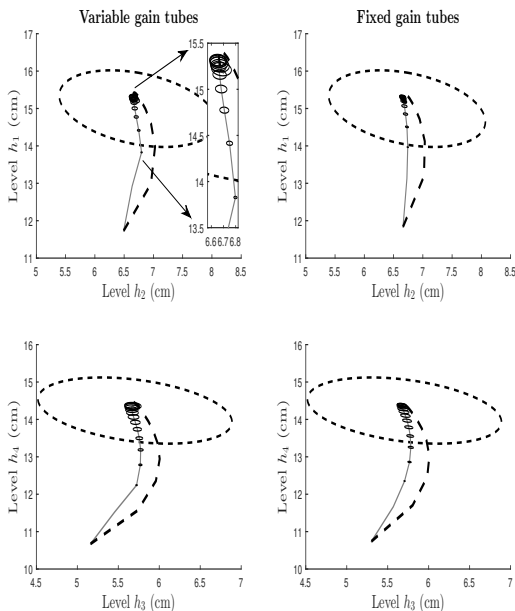


Fig. 9. A predicted trajectory for the tank levels and the tubes generated with the decentralized controller.

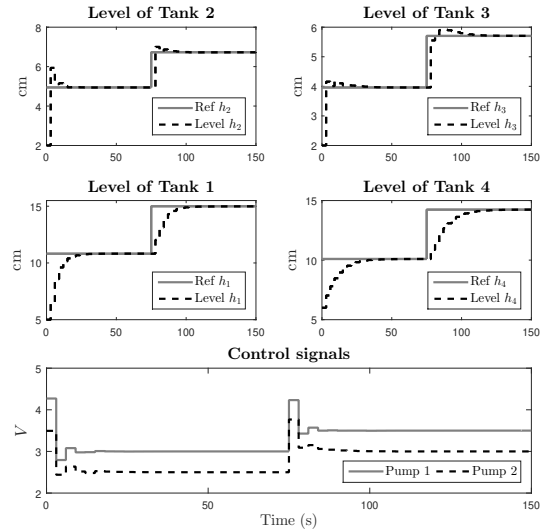


Fig. 10. Tank levels and control signals for the decentralized controller with fixed gains.

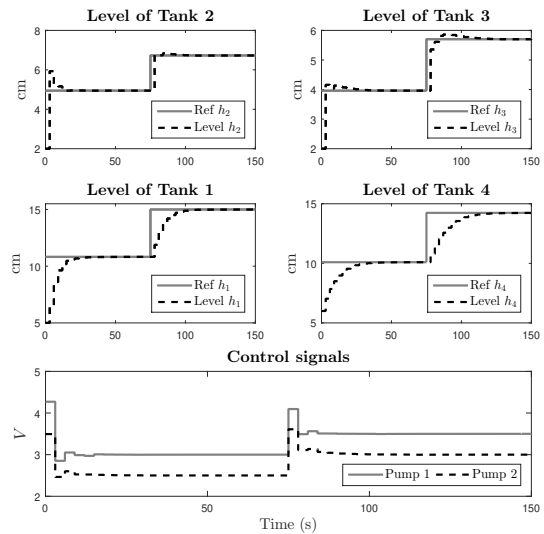


Fig. 11. Tank levels and control signals for the decentralized controller with variable gains.

In order to make a more fair comparison of the proposed controller performance, a cascade PI controllers scheme was applied. Fig. 12 depicts the PI scheme. $K_{p1} = 0.6203$, $K_{i1} = 0.0113$, $K_{p2} = 0.2219$, $K_{i2} = 2.4188 \times 10^{-4}$, $K_{p3} = 0.6203$, $K_{i3} = 0.0113$, $K_{p4} = 8.6661$, $K_{i4} = 1.7168$. Fig. 13 presents the results with the cascade PI controllers. As observed in the figure, the response obtained is too slow with these controllers, taking into account the same initial conditions and references which were established for predictive controllers.

Table 2. Costs obtained with centralized MPC, decentralized MPC and cascade PI.

Controller	J_e	J_u	J
Centralized MPC fixed gains	159.49	992.93	1152.42
Centralized MPC variable gains	159.41	993.83	1153.24
Decentralized MPC fixed gains	209.59	955.74	1165.33
Decentralized MPC variable gains	213.87	954.5	1168.37
Cascade PI controllers	2206.28	12809.21	15015.49

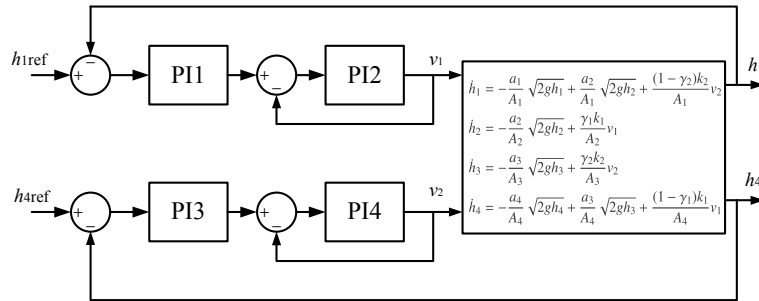


Fig. 12. Cascade PI controllers applied to the four tank system.

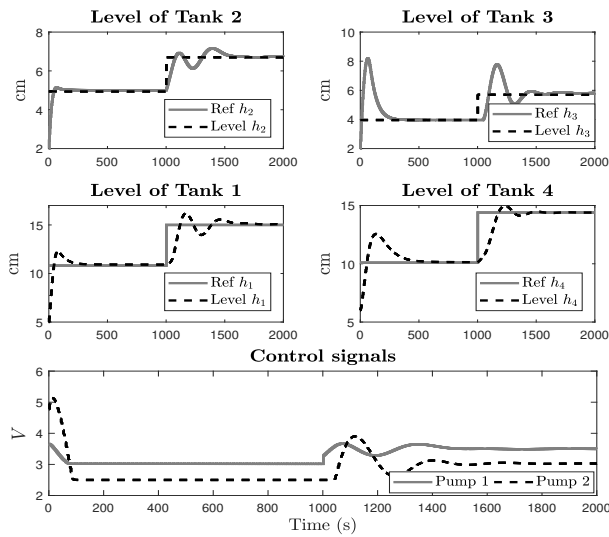


Fig. 13. Tank levels and control signals for cascade PI controllers.

A more accurate way to obtain a measure of the performance and differences between the controllers is to evaluate the following cost function

$$J = \underbrace{\sum_{k=1}^{k_f} \|\mathbf{x}_k - \mathbf{x}_{rk}\|_{\mathbf{Q}_J}^2}_{J_e} + \underbrace{\sum_{k=1}^{k_f} \|\mathbf{u}_k\|_{\mathbf{R}_J}^2}_{J_u} \quad (24)$$

where $\mathbf{Q}_J = \mathbf{I}$ and $\mathbf{R}_J = \mathbf{I}$ with \mathbf{I} as an identity matrix of proper dimensions.

Table shows the results obtained after evaluating the cost function (24) for the applied MPC controllers and cascade PI schemes. As can be seen from the table, the centralized MPC scheme has almost the same performance with respect to the decentralized MPC controller. Taking into account each term of the cost function, the centralized controller has a better performance related to the tracking error, but the centralized controller has a lower control effort. Using the centralized controller, the tank levels converge faster than the decentralized controller. This is because the centralized controller has a higher control effort. Regarding the performance of the cascade scheme, it is observed in the table that this controller has poor performance with respect to the performance of the MPC controllers. Table shows these facts.

Conclusions

In this paper, a decentralized MPC development based on robust tubes is presented. Both schemes, the centralized MPC and the decentralized MPC, were applied to a four-tank process. The numerical results show that there are slight differences between the performance of the controllers. Analyzing the cost of each controller, it was observed that the centralized controller has a higher control effort than the decentralized controller. In the case of the tracking error, the centralized controller has a better

performance than the decentralized controller. With the centralized controller, the tank levels reach the desired setpoint faster. This is because, unlike the decentralized controller, the centralized controller has complete system information at each sampling time. Regarding the performance and computational cost of each controller, controllers with fixed gain tubes have a lower computational cost than controllers with variable gain tubes, eliminating the need for the use of a more complex controller. Referring to the results obtained from the cascading PI controllers, it was observed that this control scheme could not improve the performance of the MPC controllers. This is related to the fact that classical PI controllers do not have access to complete information about the states and the interaction of control inputs. Another important fact is that PI controllers are linear. These controllers can only regulate a nonlinear system in a small region of operation.

References

- Bemporad, A., & Morari, M. Robust model predictive control: A survey. (1999) In: *Robustness in Identification and Control*, (A. Garulli and A. Tesi, eds.), Pp. 207-226. Springer, London.
- Buerger, J. (2013). Fast Model Predictive Control. PhD thesis. University of Oxford.
- Camacho, E. F., & Bordons, C. (2004). *Model Predictive Control*, Springer, Spain.
- Camponogara, E., Jia, D., & Krogh, B. (2002). Distributed model predictive control. *IEEE Control Systems Magazine* 22, 44-52. <https://doi.org/10.1109/37.980246>
- Cannon, M., Buerger, J., Kouvaritakis, B., & Raković, S. (2011). Robust tubes in nonlinear model predictive control. *IEEE Transactions on Automatic Control* 56, 1942-1947. <https://doi.org/10.1109/TAC.2011.2135190>
- Cannon, M., Kouvaritakis, B., & Desmond, N. (2009). Probabilistic tubes in linear stochastic model predictive control. *Systems & Control Letters* 58, 741-753. <https://doi.org/10.1016/j.sysconle.2009.08.004>
- Chu, T., & Chen, C. (2017). Design and implementation of model predictive control for a gyroscopic inverted pendulum. *Applied Science* 7, 1-18. <https://doi.org/10.3390/app7121272>
- Clarke, D., Mohtadi, C. & Tuffs, P. (1987). Generalized predictive control-part I. The basic algorithm. *Automatica* 23, 137-148. [https://doi.org/10.1016/0005-1098\(87\)90087-2](https://doi.org/10.1016/0005-1098(87)90087-2)
- Clarke, D., Mohtadi, C. & Tuffs, P. (1987). Generalized predictive control-part II. Extension and interpretation. *Automatica* 23, 149-160. [https://doi.org/10.1016/0005-1098\(87\)90088-4](https://doi.org/10.1016/0005-1098(87)90088-4)
- Cutler, C., & Ramaker, B. (1979). Dynamic matrix control- A computer control algorithm. In: *Proceeding of the 86th National Meeting of the American Institute of Chemical Engineers (AIChE)*. Houston, Texas.
- Gonzalez, R., Fiacchini, M., Alamo, T., Guzman, J. & Rodriguez, F. (2011). Online robust tube-based MPC for time-varying systems: a practical approach. *International Journal of Control* 84, 1157-1170. <https://doi.org/10.1080/00207179.2011.594093>
- Gonzalez, R., Fiacchini, M., Guzman, J., Alamo, T., & Rodriguez, F. (2011). Robust tube-based predictive control for mobile robots in off-road conditions. *Robotics Autonomous Systems* 59, 711-726. <https://doi.org/10.1016/j.robot.2011.05.006>
- Jia, D., & Krogh, B. (2001). Distributed model predictive control. In: *IEEE American Control Conference*, Pp. 2767-2771. Arlington, USA.
- Johansson, K. (2000). The quadruple-tank process: a multivariable laboratory with an adjustable zero. *IEEE Transactions on Control Systems Technology* 8, 456-465. <https://doi.org/10.1109/87.845876>
- Kwon, W., & Byun, D. (1989). Receding horizon tracking control as a predictive control and its stability properties. *International Journal of Control* 50, 1807-1825. <https://doi.org/10.1080/00207178908953467>
- Langson, W., Chrysochoos, I., & Raković, S. (2004). Robust model predictive control using

- tubes. *Automatica* 40, 125-133. <https://doi.org/10.1016/j.automatica.2003.08.009>
- Lee, J., Gelormino, M., & Morari, M. (1992). Model predictive control of multi-rate sample-data systems: a space-state approach. *International Journal of Control* 55, 53-191. <https://doi.org/10.1080/00207179208934231>
- Lee, J., Morari, M., & Garcia, C. (1994). Space State interpretation of model predictive control. *Automatica* 30 (4), 707-717. [https://doi.org/10.1016/0005-1098\(94\)90159-7](https://doi.org/10.1016/0005-1098(94)90159-7)
- Limon, D., Alvarado, I., Alamo, T., & Camacho, F. (2010). Robust tube-based MPC for tracking of constrained linear systems with additive disturbances. *Journal of Process Control* 20, 248-260. <https://doi.org/10.1016/j.jprocont.2009.11.007>
- Marquis, P., & Broustails, J. (1988). SMOC, a bridge between state space and model predictive controllers: application to the automation of a hydrotreating unit. In: *IFAC Model Based Procces*, Pp. 37-45. Atlanta, USA.
- Mayne, D., Kerrigan, E., & Falugi, P. (2011). Tube-based robust nonlinear model predictive control. *International Journal of Robust and Nonlinear Control* 21, 1341-1353. <https://doi.org/10.1002/rnc.1758>
- Mayne, D., Rawlings, J., & Rao, P. (1993). Constrained model predictive control: Stability and optimality. *Automatica* 36, 789-814. <https://doi.org/10.1109/9.241565>
- Mayne, D., Seron, M., & Raković, S. (2005). Robust model predictive control of constrained linear systems with bounded disturbances. *Automatica* 41, 219-224. <https://doi.org/10.1016/j.automatica.2004.08.019>
- Morari, M. (1994). Model predictive control: multivariable control technique of choice in the 1990s. In: *Control and Dynamical Systems*, (D. Clarke, ed.), Pp. 22-37. Oxford University Press, London.
- Morari, M., & Lee, J. (1999). Model predictive control: past, present and future. *Computers & Chemical Engineering* 23, 667-682. [https://doi.org/10.1016/S0098-1354\(98\)00301-9](https://doi.org/10.1016/S0098-1354(98)00301-9)
- Patwardhan, A., Rawlings, J., & Edgar, T. (1990). Nonlinear Model Predictive Control. *Chemical Engineering Communications* 87, 123-141. <https://doi.org/10.1080/00986449008940687>
- Rawlings, J., & Muske, K. (1993). The stability of constrained receding horizon control. *IEEE Transactions on Automatic Control* 38, 1512-1516. <https://doi.org/10.1109/9.241565>
- Richalet, J. (1993). *Pratique de la Commande Prédictive*. Hermes, France .
- Richalet, J., Rault, A., Testud, L., & Papon, J. (1978). Model predictive heuristic control: application to industrial processes. *Automatica* 14, 413-428. [https://doi.org/10.1016/0005-1098\(78\)90001-8](https://doi.org/10.1016/0005-1098(78)90001-8)
- Rivas-Perez, R., Sotomayor-Moriano, J., Perez-Zuñiga, C. G., & Calderon-Mendoza, E. M. (2013). Design of a multivariable gpc based on an industrial pc for control of a reverse osmosis unit of a pharmaceutical industry. *Revista Mexicana de Ingeniería Química* 15, 259-273.
- Rivero, S., & Ferrari-Trecate, G. (2012). Tube-based distributed control of linear constrained systems. *Automatica* 48, 2860-2865. <https://doi.org/10.1016/j.automatica.2012.08.024>
- Rumbo-Morales, J., Lopez-Lopez, G., Alvarado, V., Valdez-Martinez, J., Sorcia-Vázquez, F., & Brizuela-Mendoza, J. (2018). Simulation and control of a pressure swing adsorption process to dehydrate ethanol. *Revista Mexicana de Ingeniería Química* 17, 1051-1081. <https://doi.org/10.24275/uam/izt/dcbi/revmexingquim/2018v17n3/Rumbo>
- Sorcía-Vázquez, F., Garcia-Beltran, C., Valencia-Palomo, G., Guerrero-Ramírez, G., Adam-Medina, M., & Escobar-Jiménez, R. (2015). Distributed model predictive control applied to a four interconnected tank process. *Revista Iberoamericana de Informática y Automática Industrial* 12, 365-375. <https://doi.org/10.1016/j.riai.2015.07.002>
- Trodden, P., & Richards, A. (2010). Distributed model predictive control of linear systems with

persistent disturbances. *International Journal of Control* 83, 1653-1663. <https://doi.org/10.1080/00207179.2010.485280>

Trodden, P., & Richards, A. (2014). Cooperative tube-based distributed MPC for linear uncertain systems coupled via constraints. In: *Distributed Model Predictive Control Made Easy*, (J. Maestre and R. Negenbor, eds.), Pp. 57-72. Springer.

Vaccarini, M., Longhi, S., & and Katebi, M. (2009). Unconstrained networked decentralized model predictive control. *Journal of Process Control* 19, 328-339. doi: [10.1016/j.jprocont.2008.03.005](https://doi.org/10.1016/j.jprocont.2008.03.005)

Venkat, A., Hiskens, I., Rawlings, J., & Wright, S. (2008). Distributed MPC strategies with application to power system automatic generation control. *IEEE Transactions Control Systems Technology* 16, 1192-1206. <https://doi.org/10.1109/TCST.2008.919414>

Zhang, L., Xie, W., & Liu, J. (2019). Robust control of saturating systems with Markovian packet dropouts under distributed MPC. *ISA Transactions* 85, 49-59. <https://doi.org/10.1016/j.isatra.2018.08.027>

Zheng, Y., Zhou, J., Xu, Y., Zhang, Y., & Qian, Z. (2017). A distributed model predictive control based load frequency control scheme for multi-area interconnected power system using discrete-time Laguerre functions. *ISA Transactions* 68, 127-140. <https://doi.org/10.1016/j.isatra.2017.03.009>

Appendix

Centralized robust tube-based model predictive control

The centralized robust tube-based MPC design considers a global nonlinear model (Cannon M. et al., 2011).

$$\mathbf{x}_{k+1} = f(\mathbf{x}_k, \mathbf{u}_k), \quad (\text{A.1})$$

where $\mathbf{x}_k \in \mathbb{R}^n$ and $\mathbf{u}_k \in \mathbb{R}^m$ are the state and the control input, respectively. f is continuous and differentiable $\forall (\mathbf{x}, \mathbf{u})$ in a operating region and $f(0,0) = 0$. The control

problem is established as an optimal regulator with respect to the quadratic cost

$$J = \sum_{k=0}^{\infty} (\|\mathbf{x}_k\|_{\mathbf{Q}}^2 + \|\mathbf{u}_k\|_{\mathbf{R}}^2), \quad (\text{A.2})$$

subject to linear constraints of the form

$$\mathbf{F}\mathbf{x}_k + \mathbf{G}\mathbf{u}_k \leq \mathbf{h}, \quad k = 0, 1, \dots; \quad (\text{A.3})$$

for $\mathbf{F} \in \mathbb{R}^{n_u \times n}$, $\mathbf{G} \in \mathbb{R}^{n_u \times m}$, considering the state \mathbf{x}_k measured at each sample k , with $\mathbf{R} > 0$ and $\mathbf{Q} \geq 0$.

The state and the control predicted trajectories at sample k over an N -step horizon are defined by $\{\mathbf{x}_{k+i|k}^0, \mathbf{u}_{k+i|k}^0, i = 0, \dots, N-1\}$. From model (A.1), as a consequence,

$$\mathbf{x}_{k+i+1|k}^0 = f(\mathbf{x}_{k+i|k}^0, \mathbf{u}_{k+i|k}^0),$$

with $\mathbf{x}_{k|k}^0 = \mathbf{x}_k$.

The system state and control input are defined in terms of the state and control predicted trajectories

$$\mathbf{x}_{k+i|k} = \mathbf{x}_{k+i|k}^0 + \mathbf{x}_{k+i|k}^{\delta}, \quad \mathbf{u}_{k+i|k} = \mathbf{u}_{k+i|k}^0 + \mathbf{u}_{k+i|k}^{\delta},$$

for $i = 1, \dots, N-1$, with $\mathbf{x}_{k+i|k}^{\delta} = 0$, and parametrizing $\mathbf{u}_{k+i|k}^{\delta}$ as the sum of a linear feedback control law and a feedforward \mathbf{v}

$$\mathbf{u}_{k+i|k}^{\delta} = \mathbf{K}_{k+i|k} \mathbf{x}_{k+i|k}^{\delta} + \mathbf{v}_{k+i|k}. \quad (\text{A.4})$$

A centralized time-varying linear model is used to set the restrictions, described by

$$\mathbf{x}_{k+i+1|k}^{\delta} = \Phi_{k+i|k} \mathbf{x}_{k+i|k}^{\delta} + \mathbf{B}_{k+i|k} \mathbf{v}_{k+i|k} + \mathbf{w}_{k+i|k}. \quad (\text{A.5})$$

This model is derived from the linearization of the global nonlinear model (A.1) around $\mathbf{x}_{k+i|k}^0, \mathbf{u}_{k+i|k}^0$

$$\Phi_{k+i|k} = \mathbf{A}_{k+i|k} + \mathbf{B}_{k+i|k} \mathbf{K}_{k+i|k};$$

$$\mathbf{A}_{k+i|k} = \left. \frac{\partial f}{\partial \mathbf{x}_k} \right|_{\mathbf{x}_{k+i|k}^0, \mathbf{u}_{k+i|k}^0}, \quad \mathbf{B}_{k+i|k} = \left. \frac{\partial f}{\partial \mathbf{u}_k} \right|_{\mathbf{x}_{k+i|k}^0, \mathbf{u}_{k+i|k}^0},$$

and $\mathbf{w}_{k+i|k}$ is the linearization error. Matrices $\mathbf{A}_{k+i|k}$ and $\mathbf{B}_{k+i|k}$ are updated along the predicted trajectory at each step time. Predictions for $i \geq N$ are determined from the linearization of (A.1) about the target setpoint $(\mathbf{x}_k, \mathbf{u}_k) = (0,0)$ (around the state space origin), and a fixed control law $\hat{\mathbf{K}}\mathbf{x}_k$

$$\mathbf{x}_{k+i+1|k} = \hat{\Phi} \mathbf{x}_{k+i|k} + \hat{\mathbf{w}}_{k+i|k}; \quad (\text{A.6})$$

$$\mathbf{u}_{k+i|k} = \hat{\mathbf{K}}\mathbf{x}_{k+i|k}, \quad (\text{A.7})$$

for $i = N, N+1, \dots$, where $\hat{\Phi} = \hat{\mathbf{A}} + \hat{\mathbf{B}}\hat{\mathbf{K}}$, with

$$\hat{\mathbf{A}} = \left. \frac{\partial f}{\partial \mathbf{x}_k} \right|_{(0,0)}, \quad \hat{\mathbf{B}} = \left. \frac{\partial f}{\partial \mathbf{u}_k} \right|_{(0,0)}.$$

Matrices $\hat{\mathbf{A}}$ and $\hat{\mathbf{B}}$ are terminal matrices calculated off-line.

Bounds on the linearization error \mathbf{w} and $\hat{\mathbf{w}}$ can be used to bound the predicted cost and to determine robustly feasible constraints. Since f is continuous and differentiable, exists a convex set $\Omega \subset \mathbb{R}^{n \times (n+m)}$ such that $\mathbf{w}_k \in \Omega \left[\begin{matrix} \mathbf{x}_k^{\delta T} & \mathbf{u}_k^{\delta T} \end{matrix} \right]^T$. It is assumed that Ω is polytopic with vertices $\left[\begin{matrix} \mathbf{C}_j & \mathbf{D}_j \end{matrix} \right], j = 1, \dots, p$, as a result

$$\mathbf{w}_k \in \text{Co} \left\{ \mathbf{C}_j \mathbf{x}_k^{\delta} + \mathbf{D}_j \mathbf{u}_k^{\delta}, j = 1, \dots, p \right\} \quad (\text{A.8})$$

where Co denotes the convex hull. Similarly, for $i \geq N$ the errors $\hat{\mathbf{w}}_{k+i|k}$ necessarily lie within the convex set

$$\hat{\mathbf{w}}_k \in \text{Co} \left\{ \hat{\mathbf{C}}_j \mathbf{x}_k + \hat{\mathbf{D}}_j \mathbf{u}_k, j = 1, \dots, p \right\}. \quad (\text{A.9})$$

In order to bound the effects of the linearization errors on predicted trajectories, a tube is constructed containing the component of the predicted state appearing from the linearization errors. The tube is used to derive bounds on the cost and constraints in the nonlinear MPC optimization.

The prediction of $\mathbf{x}_{k+i|k}^{\delta}$ is divided into a nominal component $\mathbf{z}_{k+i|k}$ and a component $\mathbf{e}_{k+i|k}$ which depends only on the linearization $\mathbf{w}_{k+i|k}$:

$$\mathbf{x}_{k+i|k}^{\delta} = \mathbf{z}_{k+i|k} + \mathbf{e}_{k+i|k} \quad (\text{A.10a})$$

$$\mathbf{z}_{k+i+1|k} = \Phi_{k+i|k} \mathbf{z}_{k+i|k} + \mathbf{B}_{k+i|k} \mathbf{v}_{k+i|k} \quad (\text{A.10b})$$

$$\mathbf{e}_{k+i+1|k} = \Phi_{k+i|k} \mathbf{e}_{k+i|k} + \mathbf{w}_{k+i|k}, \quad (\text{A.10c})$$

with $\mathbf{z}_{k|k} = \mathbf{e}_{k|k} = 0$. The constructed tubes will have an ellipsoidal cross section

$$\mathbf{e}_{k+i|k} \in \mathcal{E}(\mathbf{V}_{k+i|k}, \beta_{k+i|k}^2), i = 1, \dots, N \quad (\text{A.11a})$$

$$\mathbf{x}_{k+i|k} \in \mathcal{E}(\hat{\mathbf{V}}, 1) i \geq N, \quad (\text{A.11b})$$

where $\mathcal{E}(\mathbf{P}, \rho^2)$, for $\mathbf{P} > 0$ denotes the ellipsoidal set $\mathcal{E}(\mathbf{P}, \rho^2) = \{ \mathbf{x} : \mathbf{x}^T \mathbf{P} \mathbf{x} \leq \rho^2 \}$.

From (A.11b), $\mathcal{E}(\hat{\mathbf{V}}, 1)$ is a terminal constraint set which must be invariant under (A.6) and (A.7), requiring that

$$\begin{aligned} \hat{\Phi} \mathbf{x} + \hat{\mathbf{w}} &\in \mathcal{E}(\hat{\mathbf{V}}, 1), \forall \hat{\mathbf{w}} \in \text{Co} \left\{ (\hat{\mathbf{C}}_j + \hat{\mathbf{D}}_j \hat{\mathbf{K}}) \mathbf{x} \right\}, \\ \forall \mathbf{x} &\in \mathcal{E}(\hat{\mathbf{V}}, 1). \end{aligned} \quad (\text{A.12})$$

It is also required a feasible $\mathcal{E}(\hat{\mathbf{V}}, 1)$ with respect to (A.3), in order to ensure the achievement of the input and state constraints over an infinite prediction horizon. From this consideration,

$$(\mathbf{F} + \mathbf{G} \hat{\mathbf{K}}) \mathbf{x} \leq \mathbf{h}, \forall \mathbf{x} \in \mathcal{E}(\hat{\mathbf{V}}, 1). \quad (\text{A.13})$$

In order to obtain the matrices $\hat{\mathbf{K}}$ and $\hat{\mathbf{V}}$, a semidefinite program (SDP) is solved off-line to maximize the local terminal set $\mathcal{E}(\hat{\mathbf{V}}, 1)$ subject to (A.12) and (A.13). Thus, being $\hat{\mathbf{S}}_i, \hat{\mathbf{Y}}_i$ the problem solution:

$$\begin{aligned} &\max_{\hat{\mathbf{S}}, \hat{\mathbf{Y}}} \det(\hat{\mathbf{S}}) \\ &\text{s. t.} \\ &\left[\begin{matrix} \hat{\mathbf{S}} & (\hat{\mathbf{A}} + \hat{\mathbf{C}}_j) \hat{\mathbf{S}} + (\hat{\mathbf{B}} + \hat{\mathbf{D}}_j) \hat{\mathbf{Y}} \\ * & \hat{\mathbf{S}} \end{matrix} \right] \geq 0, j = i, \dots, p \\ &\left[\begin{matrix} \mathbf{h}_q^2 & \mathbf{F}_q \hat{\mathbf{S}} + \mathbf{G}_q \hat{\mathbf{Y}} \\ * & \hat{\mathbf{S}} \end{matrix} \right] \geq 0, q = 1, \dots, n_c, \end{aligned} \quad (\text{A.14})$$

then the volume of $E(\hat{\mathbf{V}}, 1)$ is maximized with $\hat{\mathbf{V}} = \hat{\mathbf{S}}^{-1}$ y $\hat{\mathbf{K}} = \hat{\mathbf{Y}} \hat{\mathbf{S}}^{-1}$. Notice that $[\cdot]_q$ denotes the q th row of $[\cdot]$.

Two different types of tubes can be constructed: (i) time-varying cross section tubes and feedback gains and, (ii) fixed cross section tubes and feedback gains. In order to construct a time-varying tube and feedback gains, the following SPD in variables $\mathbf{S}, \mathbf{Y}, \gamma$ is defined

$$\begin{aligned} &\max_{\mathbf{S}, \mathbf{Y}, \gamma} \gamma \\ &\text{s. t.} \\ &\mathbf{S} \geq \gamma \mathbf{I} \\ &\left[\begin{matrix} \mathbf{S} & (\mathbf{A}_{k+i|k} + \mathbf{C}_j) \mathbf{S} + (\mathbf{B}_{k+i|k} + \mathbf{D}_j) \mathbf{Y} \\ * & \mathbf{V}_{k+i|k}^{-1} \end{matrix} \right] \geq 0, \\ &j = i, \dots, p, \end{aligned} \quad (\text{A.15})$$

as a result, by considering $\mathbf{V}_{k+i|k} = \mathbf{S}^{-1}$, $\mathbf{K}_{k+i|k} = \mathbf{Y} \mathbf{S}^{-1}$, the variable cross section tubes are computed. The fixed cross section tubes, on the other hand, are obtained by defining $\mathbf{V}_{k+i|k} = \hat{\mathbf{V}}$, $\mathbf{K}_{k+i|k} = \hat{\mathbf{K}}$.

The cost function to optimize is

$$J(\mathbf{x}_k, \mathbf{u}_k) = \sum_{k=0}^{N-1} \left(\|x_{k+i|k}\|_{\mathbf{Q}}^2 + \|u_{k+i|k}\|_{\mathbf{R}}^2 \right) + \|x_{k+N|k}\|_{\mathbf{P}}^2, \quad (\text{A.16})$$

where \mathbf{P} is computed off-line from

$$\begin{aligned} &\min_{\mathbf{P}} \text{tr}(\mathbf{P}) \\ &\text{s. t.} \\ &\mathbf{P} - (\hat{\Phi} + \hat{\mathbf{C}}_j + \hat{\mathbf{D}}_j \hat{\mathbf{K}})^T \mathbf{P} (\hat{\Phi} + \hat{\mathbf{C}}_j + \hat{\mathbf{D}}_j \hat{\mathbf{K}}) \geq \mathbf{Q} + \hat{\mathbf{K}}^T \mathbf{R} \hat{\mathbf{K}}, \\ &j = 1, \dots, p, \end{aligned} \quad (\text{A.17})$$

The cost function (A.16) is divided into individual

terms $l_{x,i}$, $l_{u,i}$, for $i = 0, \dots, N - 1$, and $l_{x,N}$

$$l_{x,i} = \left\| \mathbf{x}_{k+i|k}^0 + \mathbf{z}_{k+i|k} \right\|_{\mathbf{Q}} + \beta_{k+i|k} \left\| \mathbf{V}_{k+i|k}^{-1/2} \right\|_{\mathbf{Q}} \quad (\text{A.18a})$$

$$l_{u,i} = \left\| \mathbf{u}_{k+i|k}^0 + \mathbf{K}_{k+i|k} \mathbf{z}_{k+i|k} + \mathbf{v}_{k+i|k} \right\|_{\mathbf{R}} \quad (\text{A.18b})$$

$$+ \beta_{k+i|k} \left\| \mathbf{K}_{k+i|k} \mathbf{V}_{k+i|k}^{-1/2} \right\|_{\mathbf{R}} \quad (\text{A.18c})$$

$$l_{x,N} = \left\| \mathbf{x}_{k+N|k}^0 + \mathbf{z}_{k+N|k} \right\|_{\mathbf{P}} + \beta_{k+N|k} \left\| \hat{\mathbf{V}}^{-1/2} \right\|_{\mathbf{P}} \quad (\text{A.18d})$$

Finally, the solution of the centralized MPC is obtained by solving the following optimization problem

$$(\mathbf{v}_k^*, \beta_k^*) = \min_{\mathbf{v}_k, \beta_k} \sum_{i=0}^{N-1} (l_{x,i}^2 + l_{u,i}^2) + l_{x,N}^2 \quad (\text{A.19a})$$

s. t.

$$\mathbf{z}_{k+i+1|k} = \Phi_{k+i|k} \mathbf{z}_{k+i|k} + \mathbf{B}_{k+i|k} \mathbf{v}_{k+i|k} \quad (\text{A.19b})$$

$$\beta_{k+i+1|k} \geq \lambda_{i,j} \beta_{k+i} + \left\| (\mathbf{C}_j + \mathbf{D}_j \mathbf{K}_{k+i|k}) \mathbf{z}_{k+i|k} + \mathbf{D}_j \mathbf{v}_{k+i|k} \right\| \quad (\text{A.19c})$$

$$l_{u,i} \geq \left\| \mathbf{u}_{k+i|k}^0 + \mathbf{K}_{k+i|k} \mathbf{z}_{k+i|k} + \mathbf{v}_{k+i|k} \right\|_{\mathbf{R}}$$

$$+ \beta_{k+i|k} \left\| \mathbf{K}_{k+i|k} \mathbf{V}_{k+i|k}^{-1/2} \right\|_{\mathbf{R}} \quad (\text{A.19d})$$

$$\mathbf{h}_q \geq (\mathbf{F}_q \mathbf{x}_{k+i|k}^0 + \mathbf{G}_q \mathbf{u}_{k+i|k}^0) + (\mathbf{F}_q + \mathbf{G}_q \mathbf{K}_{k+i|k}) \mathbf{z}_{k+i|k} + \mathbf{G}_q \mathbf{v}_{k+i|k} + \beta_{k+i|k} \left\| (\mathbf{F}_q + \mathbf{G}_q \mathbf{K}_{k+i|k}) \right\|_{\mathbf{V}_{k+i|k}^{-1}} \quad (\text{A.19e})$$

for $i = 1, \dots, N - 1$, and

$$\mathbf{z}_{k|k} = 0 \quad (\text{A.19f})$$

$$\beta_{k|k} = 0 \quad (\text{A.19g})$$

$$1 \geq \left\| \mathbf{x}_{k+N|k}^0 + \mathbf{z}_{k+N|k} \right\|_{\hat{\mathbf{V}}} + \beta_{k+N|k} \quad (\text{A.19h})$$

$$l_{x,N} \geq \left\| \mathbf{x}_{k+N|k}^0 + \mathbf{z}_{k+N|k} \right\|_{\mathbf{P}} + \beta_{k+N|k} \left\| \hat{\mathbf{V}} \right\|_{\mathbf{P}} \quad (\text{A.19i})$$

where $\lambda_{i,j} = 1$ if a variable tube cross sections are used or $\lambda_{i,j} = \left\| \Phi_{k+i|k} \hat{\mathbf{V}}^{-1/2} \right\|_{\hat{\mathbf{V}}} + \left\| (\mathbf{C}_j + \mathbf{D}_j \hat{\mathbf{K}}) \hat{\mathbf{V}}^{-1/2} \right\|_{\hat{\mathbf{V}}}$ if a fixed tube cross sections are used.